# Comparative Evaluation of Two Registration-based Segmentation Algorithms: Application to Whole Heart Segmentation in CT

M. Unberath[1,2,3], A. Maier[1,3], D. Fleischmann[4], J. Hornegger[1,3], and R. Fahrig [2]

[1]Pattern Recognition Lab, FAU Erlangen-Nürnberg, Erlangen, Germany
[2]Radiological Sciences Laboratory, Stanford University, Stanford, USA
[3]Graduate School in Advanced Optical Technologies, FAU Erlangen-Nürnberg, Erlangen, Germany
[4]Diagnostic Radiology, Stanford University, Stanford, USA

*Abstract-* **Statistical shape models learn valid variability from example shapes, making large training sets favorable. Methods for automatic training set generation use transforms obtained by registration to propagate atlas landmarks to new samples. Algorithms based on B-spline transforms and mutual information (MI) were successfully employed for the cardiac anatomy in CT and MRI. For single-modality data, however, computationally less complex algorithms such as Thirion's Demons can be used, allowing for reduced computation times. We implemented two multi-resolution registration-based segmentation pipelines based on Thirion's Demons, and MI-driven B-spline transforms, respectively, fixed the parameters, and evaluated their performance in whole heart segmentation of contrasted CT angiography images. The segmentation quality was assessed qualitatively using visual inspection and quantitatively using expert ratings. While the Demons-based algorithm required less computation time, the results of the B-spline-based pipeline were in better agreement with the tested data and achieved a higher expert score ($3.33 \pm 0.51$ compared to $2.19 \pm 0.45$). We found registration using B-spline transforms and MI to be favorable, as the application is not time-sensitive.**

*Keywords-* **Registration, Statistical Shape Model, Automatic Segmentation, Heart Modelling, CT**

## I. INTRODUCTION

The significance of statistical shape models (SSMs) is largely dependent on their training sets. Training set generation implies segmentation of sufficiently many, representative shapes. Establishing point correspondence among all samples is imperative but challenging [8]. Registration-based segmentation algorithms avoid this problem by propagating landmarks from an atlas segmentation to unseen images using coordinate transforms obtained by image registration.

Frangi *et al.* propagated landmarks from an atlas image to manually segmented images by non-rigid registration of segmentation masks [2]. The need for manual segmentation of all input data imposes a practical limitation on the size of the training set. To overcome this limitation, Ordas *et al.* directly operate on intensity images using free-form deformations and mutual information (MI) [6]. While algorithms using B-spline transforms and MI have been shown capable of dealing with large inter-subject and temporal variability of the cardiac anatomy [10], they require optimization of a complex similarity metric in high-dimensional parameter space. For intra-modality registration, however, the mean squares metric and Thirion's Demons [9] can be employed, leading to decreased computational complexity and therefore computation time.

We implemented two registration-based segmentation pipelines using Thirion's Demons, and MI-driven B-spline transforms, respectively, and evaluated their performance in automatic cardiac segmentation. All algorithms are implemented in C++ using the Insight Toolkit (ITK) [4].

## II. MATERIALS AND METHODS

The initial segmentation was performed manually on a retrospectively gated contrasted coronary angiography CT scan of a 45 year old female at best diastolic phase ($78\%$). The reconstructed volume has $512 \times 512 \times 241$ voxels with a voxel-size of $0.29 \times 0.29 \times 0.5\,mm$. We segmented the descending aorta, right atrium and ventricle, left atrium and ventricle, and left ventricular myocardium.

The discussed algorithms both have the same structure outlined below:

- Bilateral Filtering,
- Rigid image registration using a similarity transform,
- Non-rigid image registration using multiple resolution levels,
- Propagation of the atlas segmentation.

Preprocessing and atlas propagation is similar in both pipelines, but registration steps are substantially different. All objective functions are optimized using gradient-descent.

### A. Demons-based Pipeline

This registration pipeline is suitable for intra-modality registration, as it assumes that homologous points are represented by the same intensity. Using the mean-squares metric, the objective function of the rigid registration with transform

$\mathscr{T}$ reads:

$$\arg\min_{\mathscr{T}} MS(f,m,\mathscr{T}) = \arg\min_{\mathscr{T}} \frac{1}{N}\sum_{i=1}^{N}\left(f(x_i)-m(\mathscr{T}(x_i))\right)^2, \tag{1}$$

where $f$ and $m$ are the fixed and moving image, respectively, $x_i$ is the physical position of the $i^{th}$ pixel in the fixed image, and $N$ is the number of samples considered. For rigid registration $\mathscr{T}$ is a similarity transform allowing for rotation $R \in \mathbb{R}^{n\times n}$, translation $t \in \mathbb{R}^n$, and isotropic scaling $\sigma$:

$$\mathscr{T}(x) = Rx + t, \tag{2}$$

such that $\det(R) = \sigma^n$. We used 10% of the fixed image pixels and 300 iterations. Rigid registration is followed by Thirion's Demons algorithm on four scale-space levels. The algorithm iteratively updates an initial displacement field $D_0(x)$. The updates are calculated using optical flow and the local image gradient followed by renormalization:

$$D(x) = -\frac{(m(x)-f(x))\,\nabla f(x)}{\|\nabla f(x)\|^2 + (m(x)-f(x))^2/K}, \tag{3}$$

where $K$ is a normalization factor. For greater detail refer to [9]. The resulting deformation field is smoothed with a Gaussian kernel with a standard deviation of $1.2\,mm$ after each iteration. The number of iterations were 1500, 1200, 750 and 150 from coarse to fine. The runtime of 1 h 49 min was measured for the registration of a volumetric image with $512\times512\times241$ pixels to the initially segmented volume on a $64\,Bit$ Windows 7 laptop equipped with an Intel® Core™ i7-3632QM operating at $2.20\,GHz$ and $8\,GB$ RAM. Implementations of the Demons algorithm on the GPU are available allowing for significant acceleration.

### *B. B-spline-based Pipeline*

Using MI as the similarity metric allows for intra- but also for inter-modality registration as no assumptions about intensity correlations are made. Using MI, however, increases computational complexity and hence computation time. Assuming a transform $\mathscr{T}$, one has to optimize:

$$\begin{aligned} &\arg\max_{\mathscr{T}} MI(f,m,\mathscr{T}) \\ &= \arg\max_{\mathscr{T}} \sum_{i,j} p_{fm}\left(f(x_i), m(\mathscr{T}(x_j))\right)\cdots \\ &\qquad \log\left(\frac{p_{fm}\left(f(x_i), m(\mathscr{T}(x_j))\right)}{p_f\left(f(x_i)\right)\, p_m\left(m(\mathscr{T}(x_j))\right)}\right), \end{aligned} \tag{4}$$

where $p_f$ and $p_m$, and $p_{fm}$ are the marginal and joint probability density functions (i.e. histograms) of the fixed and moving image, respectively. Derivations can be found in [5].

For rigid registration, we combine the objective function in Eq. 4 with the transform defined in Eq. 2. We use 70 histogram bins and 10% of the central fixed image pixels for the calculation of MI, and 150 iterations for optimization.

Free form models deform an object by manipulating an underlying mesh of control points and can be connected to any similarity metric. Higher dimensional deformations can be written as the tensor product of 1D cubic B-Splines defined on the domain $0 < x < x_{max}$:

$$\mathscr{T}(x) = \sum_{n=0}^{3} B_n(u)\Phi_{k+n}, \tag{5}$$

where $k = \lfloor \frac{x}{n_x} \rfloor - 1$, $u = \frac{x}{n_x} - \lfloor \frac{x}{n_x} \rfloor$, $n_x$ is the number of control points $\Phi_i$ in that direction and $B_n(u)$ represents the $n^{th}$ cubic B-spline basis function [7]. We used 4, 9, 13, and 18 grid nodes with 300, 250, 200, and 150 iterations in the coarse to fine resolution scheme. 70 histogram bins and 10% of the fixed image pixels were used for the estimation of the underlying probability density functions. Using the hardware described above the runtime was 2 h 21 min.

## III.RESULTS

We evaluate the performance of both pipelines by comparing the resulting segmentation accuracy. Findings will be motivated using representative data sets of a female patient's heart at end diastole and a male patient's heart at end systole. Results obtained with the Demons-based pipeline are consistently worse compared to the ones obtained with the B-spline-based approach. The segmentation of left ventricle, and myocardium is of similar accuracy in the female patient's data set (c.f. Fig. 1(a) and 1(d)). In both cases, however, the myocardium extends too far into the surrounding tissue (emphasized in Fig. 1(a)). The boundary between aorta and left ventricle is inaccurately determined with Demons-based segmentation. The most significant error can be observed in Fig. 1(d), where the delineation of the right atrium extends into the aorta and left ventricle. Neither error can be observed in the B-spline-based segmentation in this data set.

For the male patient's data set, the segmentation of the right atrium is not very accurate in the B-spline case, however, it is worse for the Demons pipeline (evident in Fig. 1(b) and 1(e)). The right atrium comprises great vessels while parts of the right ventricle are shifted into the right atrium in both cases (not shown). The Demons-based algorithm gives particularly incorrect delineations of left atrium and ventricle, and myocardium. The erroneous segmentation leads to larger left ventricular and myocardial volumes (refer to Fig. 1(e)).

Three experts were asked to independently judge segmentation quality of both pipelines for all ten acquired phases of the cardiac cycle on a scale from 0 to 5, where 5 indicates perfect segmentation accuracy and 0 indicates erroneous delineation of all anatomical components. The results are shown in Table 1.

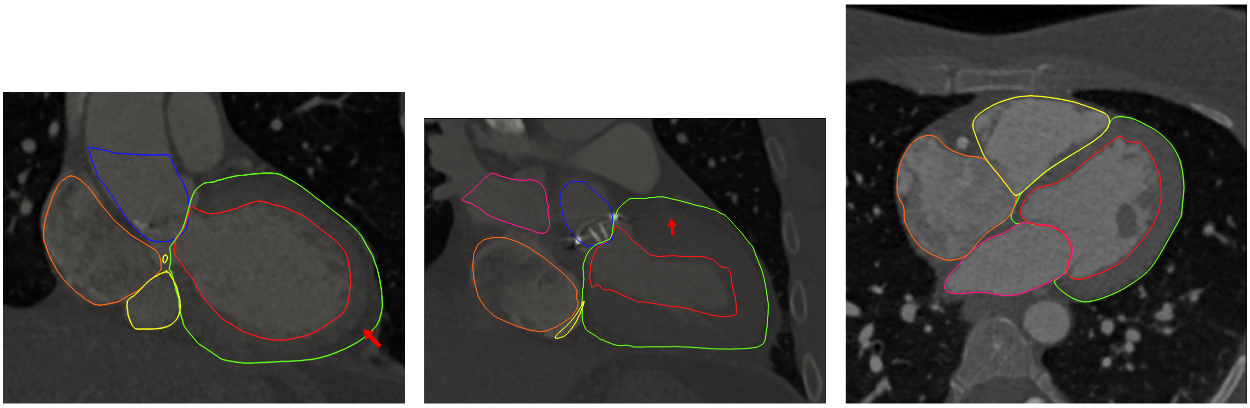

(a) Female, B-splines: Coronal view (b) Male, B-splines: Coronal view (c) Ground truth segmentation: Axial view

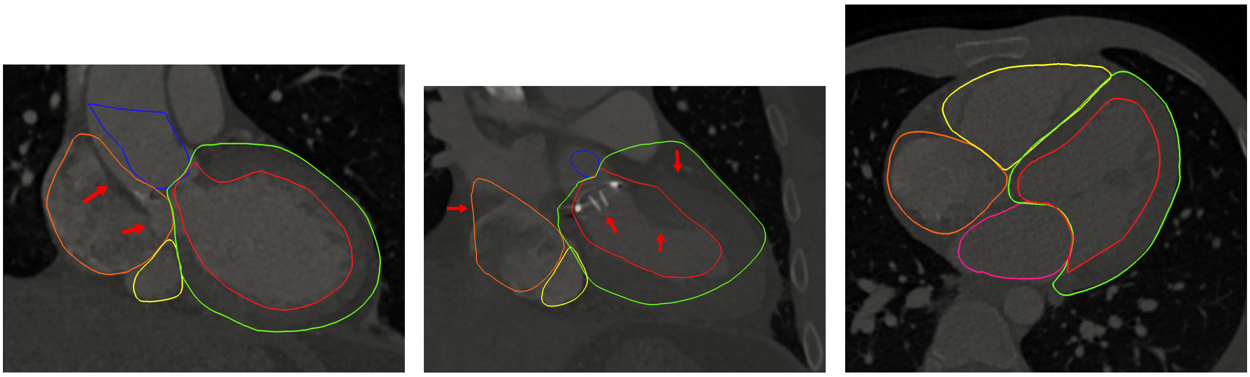

(d) Female, Demons: Coronal view (e) Male, Demons: Coronal view (f) B-Splines, Best case scenario: Axial view

Fig. 1 Segmentation results for the female patient's heart at end diastole: 1(a) 1(d), the male patient's heart: 1(b) 1(e), the ground truth segmentation: 1(c), and an optimal segmentation result obtained with the B-spline pipeline: 1(f).

## IV.DISCUSSION AND CONCLUSION

We compared the performance of two registration-based segmentation algorithms in automatic whole heart segmentation.

Results of the Demons-based pipeline indicated poor performance for marginally separated structures, such as the right atrium and ventricle. We observed erroneous segmentations of such structures in all samples. The displacements are derived from optical flow, which inherently assumes that corresponding pixels are of constant intensity in all images. In the present case, every pixel associated with blood has similar intensities and is hence equivalent in the sense of optical flow computation. The minimalistic regularization of the displacement field (Gaussian smoothing) was not sufficient to obtain correct mappings.

We found segmentations obtained with the B-spline pipeline to be more satisfactory. Although we observed similar problems with marginally separated anatomical structures, segmentations of the right and left ventricular blood pool mostly were in good agreement with the tested data. Misalignments, in particular the ones observed with the myocardium (c.f. Fig. 1(b)), can likely be explained by too coarse binning of the histograms, making discrimination of structures with similar intensities impossible. Due to the finite support region, B-spline transform deformations are smooth. In agreement with [6], the study indicated that B-spline transforms can cope with inter-subject and temporal variability.

Global contrast induced variations of blood pool intensity (compare 1(a) and 1(c)) can have significant impact on mean squares-based registrations. MI-based registrations, however, are largely unaffected. This allows for consistent segmentation quality over the cardiac cycle in the presence of contrast agent washout. Local variations in contrast agent concentration, however, can drastically influence both metrics. Strong intensity variations due to contrast enhancement were observed especially in the right atria.

Segmentation accuracy was similar in all data sets, suggesting that the initial rigid registration can sufficiently explain variations in size and pose. The evaluation indicated improved segmentation accuracy for the diastolic phases. This effect arises from the use of an initial segmentation of a data set at end diastole, biasing segmentations towards this heart state (see Table 1). While the Demons-based pipeline allowed for shorter computation times (acceleration on the GPU possible), the B-spline-based pipeline provided more accurate segmentations. As this particular use-case was not time-sensitive, MI-driven registration using B-spline trans-

Table 1 Scores on a scale from 0 to 5 for the segmentation results of both pipelines.

| | 00% | 10% | 20% | 30% | 40% | 50% | 60% | 70% | 80% | 90% |
|---|---|---|---|---|---|---|---|---|---|---|
| B-spline: | $3.67 \pm 0.61$ | $3.25 \pm 0.52$ | $3.25 \pm 0.76$ | $2.75 \pm 0.88$ | $2.25 \pm 0.69$ | $3.25 \pm 0.69$ | $3.67 \pm 0.52$ | $3.50 \pm 0.63$ | $3.75 \pm 0.42$ | $3.92 \pm 0.49$ |
| Demons: | $2.58 \pm 0.58$ | $2.08 \pm 0.74$ | $2.00 \pm 0.00$ | $1.67 \pm 0.52$ | $1.42 \pm 0.49$ | $2.08 \pm 0.20$ | $2.25 \pm 0.27$ | $2.33 \pm 0.26$ | $2.58 \pm 0.58$ | $2.92 \pm 0.66$ |

forms was favorable.

The pipelines were designed with automatic segmentation in mind. Therefore, the respective registration parameters have not been fine-tuned to each data set, implying average segmentation performance in above examples. Figure 1(f) suggests that very accurate segmentations are possible, if the registration parameters perfectly match the images to be registered.

Parameter choice is a trade-off between segmentation accuracy and computation time. Future research could focus on fine-tuning registration parameters at run-time similar to [3]. Neither pipeline currently uses prior knowledge. Shape similarity metrics between transformed and initial mesh could be introduced as regularization of the registration and knowledge about shape changes during the cardiac cycle could be exploited. Regularization might also be employed to cope with the erroneous segmentation of low contrast separations between anatomical structures, which would drastically improve segmentation quality [1]. The proposed registration-based segmentation pipeline using B-spline transforms and MI is not only applicable to automatic whole heart segmentation, but can easily be adapted to other segmentation problems, provided that an initial segmentation is available.

## ACKNOWLEDGMENT

The authors gratefully acknowledge funding of the Erlangen Graduate School in Advanced Optical Technologies (SAOT) by the German Research Foundation (DFG) in the framework of the German excellence initiative.

## REFERENCES

[1] V. Daum. *Model-Constrained Non-Rigid Registration in Medicine*. PhD thesis, Friedrich-Alexander-Universität, 2011.

[2] A. F. Frangi, D. Rueckert, J. A. Schnabel, and W. J. Niessen. Automatic construction of multiple-object three-dimensional statistical shape models: Application to cardiac modeling. *Medical Imaging, IEEE Transactions on*, 21(9):1151–1166, 2002.

[3] D. Hahn, V. Daum, and J. Hornegger. Automatic Parameter Selection for Multi-Modal Image Registration. *IEEE Transactions on Medical Imaging*, 29(5):1140–1155, 2010.

[4] L. Ibanez, W. Schroeder, L. Ng, and J. Cates. The ITK software guide. 2003.

[5] D. Mattes, D. R. Haynor, H. Vesselle, T. K. Lewellyn, and W. Eubank. Nonrigid multimodality image registration. *Medical Imaging*, pages 1609–1620, 2001.

[6] S. Ordas, E. Oubel, R. Leta, F. Carreras, and A. F. Frangi. A statistical shape model of the heart and its application to model-based segmentation. In *Medical Imaging*, pages 65111K–65111K. International Society for Optics and Photonics, 2007.

[7] D. Rueckert, L. I. Sonoda, C. Hayes, D. L. Hill, M. O. Leach, and D. J. Hawkes. Nonrigid registration using free-form deformations: application to breast MR images. *Medical Imaging, IEEE Transactions on*, 18(8):712–721, 1999.

[8] M. Spiegel, D. Hahn, V. Daum, J. Wasza, and J. Hornegger. Segmentation of kidneys using a new active shape model generation technique based on non-rigid image registration. *Computerized Medical Imaging and Graphics*, 33:29–39, 2009.

[9] J.-P. Thirion. Non-rigid matching using demons. In *Computer Vision and Pattern Recognition, 1996. Proceedings CVPR'96, 1996 IEEE Computer Society Conference on*, pages 245–251. IEEE, 1996.

[10] M. Unberath, A. Maier, D. Fleischmann, J. Hornegger, and R. Fahrig. Open-source 4D Statistical Shape Model of the Heart for X-ray Projection Imaging. In *Biomedical Imaging: From Nano to Macro, 2015 IEEE International Symposium on*. IEEE, to appear 2015.